Proceedings of the 2nd International Congress APMAS2012, April 26–29, 2012, Antalya, Turkey

Effects of Substrate Temperature on Structural Properties of Tin Oxide Films Produced by Plasma Oxidation after Thermal Evaporation

M. Alaf*, M.O. Guler, D. Gultekin and H. Akbulut
Sakarya University, Dept. of Metallurgical & Materials Engineering, 54187, Sakarya, Turkey

In this study, tin film was thermally evaporated onto a stainless steel substrate in an argon atmosphere. The tin films were then subjected to a DC plasma oxidation process using an oxygen/argon gas mixture. Three different substrate temperatures (100 °C, 150 °C, and 200 °C) and three different oxygen partial pressures (12.5%, 25%, and 50%) were used to investigate the physical and microstructural properties of the films. The surface properties were studied by scanning electron microscopy, X-ray diffraction, atomic force microscopy and a four-point probe electrical resistivity measurement. The grain size and texture coefficient of the tin oxide films were calculated. Both SnO and SnO_2 films with grain sizes of 13–43 nm were produced, depending on the oxygen partial pressure. SnO films have flower- and flake-like nanostructures, and SnO_2 films have grape-like structures with nanograins. The resistivity values for the SnO_2 phase were found to be as low as 10^{-5} Ω cm and were observed to decrease with increasing substrate temperature.

DOI: 10.12693/APhysPolA.123.326
PACS: 64.70.fm, 73.61.At, 81.16.Pr

1. Introduction

There are two main oxides of tin: stannic oxide (SnO_2) and stannous oxide (SnO). The existence of these two oxides reflects the dual valency of tin, which has oxidation states of 2+ and 4+. The applications of tin oxides include their use as catalysts, gas sensors, heat reflection filters, transparent conducting coatings, and anode materials [1]. One of the semiconducting oxide materials, SnO, has received increased attention because it is known to be a p-type semiconductor with a wide band gap ($E_g = 2.5 \div 3.0$ eV), whereas most oxide semiconductors have n-type features.

Recently, SnO has been studied as an anode material for Li-ion batteries because the capacity of SnO surpasses that of graphite or SnO_2. Because SnO is unstable at temperatures over 270 °C, in contrast with SnO_2, the former is simply reported as a precursor or an intermediate phase in the process of fabricating the SnO_2 nanostructures [2].

In this study, pure metallic tin was evaporated onto stainless steel substrates in an argon atmosphere at a pressure of 1.0 Pa, and the deposited films have been oxidized with dc (direct current) plasma in an Ar/O_2 gas mixture. The effect of substrate temperature and oxygen partial pressure on the morphology, structure, and physical properties of the films was investigated. The goal of this work is to develop an authentic method with which to produce and characterize nanosized tin oxide films that is low-cost and that provides an easy way to control the film properties.

*corresponding author

2. Experiment details

SnO and SnO_2 films were manufactured in two steps: thermal evaporation and dc plasma oxidation in a multifunctional magnetron sputtering physical vapor deposition (PVD) unit. The thin films were deposited onto cleaned and polished 316L stainless steel substrates. First, high purity metallic tin (99.999%) was placed in a Mo boat in the deposition chamber, which was evacuated to 10^{-4} Pa by a turbomolecular pump and then backfilled with argon to a pressure of 1 Pa. In the second step, SnO and SnO_2 thin films have been produced by dc plasma oxidation from the thermally evaporated tin films. The plasma oxidation of the tin films was conducted using a high-purity oxygen (99.999%) and argon (99.9999%) gas mixture. Three different substrate temperatures of 100 °C, 150 °C, and 200 °C and three different oxygen partial pressures of 12.5%, 25%, and 50% (the rest of the mixture is argon), all with a dc power of 80 W, were chosen for plasma oxidation. The oxidation time and total chamber pressure for each oxidation were kept constant at 1 h and 1.6 Pa.

An X-ray diffractometer (Rigaku D/MAX 2000), scanning electron microscopy (JEOL 6060LV) and atomic force microscopy (Quesant) and a four-point probe resistivity measurement (Bellsonics PRO4) using a WC probe has been used to characterization of the films. The grain sizes of the thin films were calculated using Scherrer's formula. Texture coefficients (TC) can be determined according to the formula [3]:

$$\mathrm{TC}(hkl) = \frac{I(hkl)/I_0(hkl)}{\sum_N I(hkl)/I_0(hkl)}, \quad (1)$$

where $I_0(hkl)$ and $I(hkl)$ are the standard X-ray intensity of the SnO_2 powder and the measured X-ray intensity, and N is the reflection number.

3. Results and discussion

3.1. Thermal evaporation of Sn coatings

Figure 1 shows a scanning electron microscopy (SEM) image and a typical X-ray diffraction (XRD) pattern for the pure tin (Sn) films evaporated onto the stainless steel substrates in an argon atmosphere at a pressure of 1.0 Pa (JCPDS file no. 01-086-2264 for powder Sn). No obvious reflection peaks from impurities were detected, providing evidence of the high purity of the product. The (220), (211) and (200) peaks are the strongest peaks observed for the film evaporated onto a stainless steel substrate in a 1.0 Pa argon atmosphere.

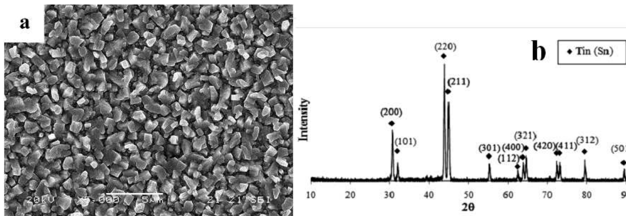

Fig. 1. (a) SEM images, (b) XRD pattern of pure tin (Sn) film evaporated at 1 Pa Ar.

In our previous study [4], we deposited tin using three different argon pressures of 0.5 Pa, 1.0 Pa, and 1.5 Pa. For the lowest chamber pressure, the strongest peak was the (200) orientation. When the pressure was increased, the preferred orientation changed from (200) to (220). Texture coefficients are 0.27, 0.1, 1.67, and 0.72 for the (200), (101), (220), and (211) planes, respectively. After thermal evaporation onto a stainless steel substrate, tin exhibits a crystalline microstructure with epitaxial grains. The calculated grain size with Scherrer's formula of the tin film that was thermally evaporated in a 1.0 Pa Ar atmosphere is 34 nm.

3.2. DC plasma oxidation

After the thermal evaporation process, the tin samples were subjected to a plasma oxidation process at three different oxygen partial pressures of 12.5%, 25%, and 50% and three different substrate temperatures of 100 °C, 150 °C, and 200 °C to produce tin oxide films. Figure 2 presents the XRD patterns of the SnO and SnO_2 films. The XRD patterns of the tin oxide films produced in a 12.5% O_2 plus 87.5% Ar atmosphere at three different substrate temperatures are presented in Fig. 2a. The films have an SnO structure, which agrees well with the standard data files (JPDS 01-072-1012), and all of the films have a crystalline structure. The XRD patterns show that the SnO nanostructures had preferred orientations of (110) and (101). The same preferred orientation of SnO films was also observed by Shin et al. [2]. They produced nanostructured tetragonal SnO films with preferred orientations of (110) and (101) using the vapor transport process. Increasing the substrate temperature resulted in an increase in the intensity of the XRD peaks corresponding to the (110), (101) and (211) planes.

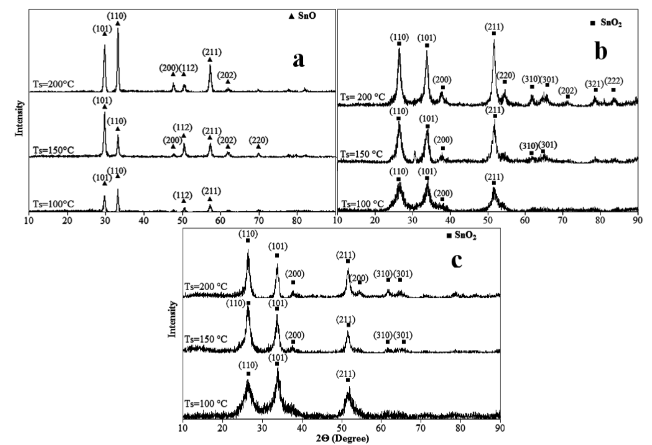

Fig. 2. XRD patterns of SnO and SnO_2 films produced at 12.5% O_2 (a), 25% O_2 (b) and 50% O_2 (c) partial pressure at three different substrate temperatures.

Table presents the textural parameters of the SnO and SnO_2 films as a function of substrate temperature. The grain sizes of the SnO films that were plasma oxidized at 12.5% O_2 partial pressure were recorded as 43.06 nm, 36.01 nm, and 29.0 nm for substrate temperatures of 100 °C, 150 °C, and 200 °C, respectively.

TABLE

Texture coefficients (TC) of SnO and SnO_2 films produced.

Substrate temperature	12.5% oxygen (SnO)					25% oxygen (SnO_2)					50% oxygen (SnO_2)			
	Planes					Planes					Planes			
	(101)	(110)	(200)	(112)	(211)	(110)	(101)	(200)	(211)	(220)	(110)	(101)	(200)	(211)
100 °C	0.34	1.81	0.31	0.35	0.64	0.43	0.93	0.66	0.91	1.03	0.42	0.90	0.22	0.59
150 °C	0.78	1.50	0.34	1.70	1.04	0.64	0.84	0.52	1.25	1.50	2.55	2.05	0.15	0.72
200 °C	0.42	2.18	0.55	0.21	1.01	0.72	0.82	0.30	1.66	1.74	1.07	1.0	0.72	1.18

The SEM images of the SnO films oxidized at 12.5% O_2 partial pressure are shown in Fig. 3 for three different substrate temperatures of 100 °C, 150 °C, and 200 °C. The SnO phase exhibited equiaxed nanograins at a sub-

strate temperature of 100 °C. Interestingly, the SnO structures appeared to have flower geometry when the substrate temperature increased to 150 and 200 °C, so these structures were called nanoflowers. In the literature it was reported that the SnO nanocrystals can exhibit different geometries, such as a branched nanostructure [2], nanoribbons [5], platelets [6], sheets [7], rossets [8], and whiskers [9], that are formed according to the production method and the deposition conditions.

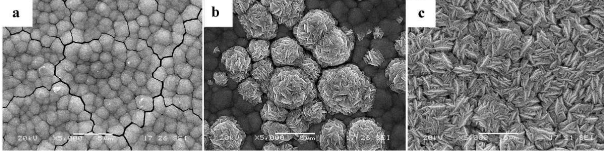

Fig. 3. SEM images of SnO films produced at 12.5% O_2 partial pressure at three different substrate temperatures (a) 100 °C, (b) 150 °C, (c) 200 °C.

AFM studies were conducted on the SnO films that were oxidized at three different substrate temperatures and they are shown in Fig. 4. AFM images were recorded from two 10×10 μm^2 areas within the films: one in the central portion of the substrate and the other at a lateral center position.

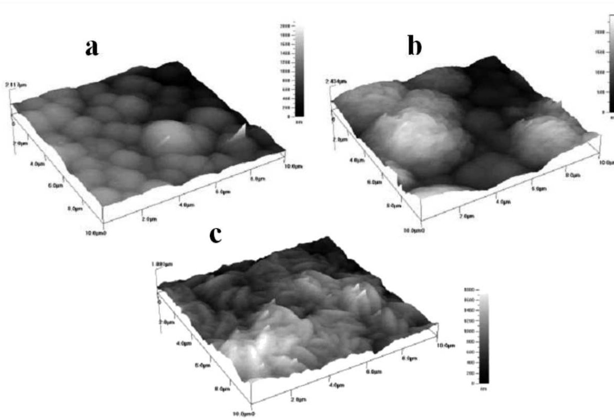

Fig. 4. AFM images of SnO films produced at 12.5% O_2 partial pressure at three different substrate temperatures (a) 100 °C, (b) 150 °C, (c) 200 °C.

The crystal structure of the plasma oxidized pure Sn depositions under the 25% and 50% O_2 partial pressure SnO_2 films was determined using the X-ray diffraction technique. All the films produced at 25% and 50% O_2 partial pressure exhibited an SnO_2 polycrystalline structure, as shown in Fig. 2b and Fig. 2c, which agrees well with the standard data files (JPDS 01-077-0447). A comparison of the SnO_2 films with the same oxygen partial pressures at different substrate temperatures shows that some crystallographic characteristics changed with temperature. As the substrate temperature increases, the crystallinity of the films improves, which is confirmed by the intensity and sharpness of the XRD peaks of the SnO_2 phase. Similar results were also reported by some researchers [9–11].

The SEM images of the SnO_2 thin films deposited by thermal evaporation from metallic tin at 1.0 Pa Ar pressure and then subsequently plasma oxidized at three different substrate temperatures and at 50% O_2 partial pressures are presented in Fig. 5. SnO_2 films plasma oxidized at 50% O_2 partial pressure are similar to the morphology presented in Fig. 5.

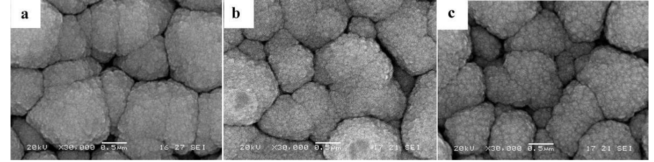

Fig. 5. SEM images of SnO_2 films produced at 25% O_2 partial pressure at three different substrate temperatures (a) 100 °C, (b) 150 °C, (c) 200 °C.

The grain sizes of the SnO_2 films that were plasma oxidized at 25% O_2 partial pressure were calculated to be 13.04 nm, 18.04 nm, and 21.6 nm for substrate temperatures of 100 °C, 150 °C, and 200 °C, respectively. A similar trend in the increase of grain size was also obtained for the SnO_2 films produced at 50% O_2 partial pressure (13 nm, 17.37 nm, and 23.7 nm). In conclusion, the grain sizes of the SnO_2 films that were plasma oxidized at 25% and 50% O_2 partial pressure increased as the substrate temperature increased.

3.3. Resistivity

The electrical resistivity of the thin films was measured by a four-point probe resistivity measurement using a WC probe. Because the SnO phase exhibited high resistivity, the test apparatus has failed to measure the resistivity values for the samples that were plasma oxidized at 12.5% and 25% O_2 partial pressure at substrate temperatures of 100 °C and 150 °C. The resistivity values that were measured for the samples that were plasma oxidized at 12.5% and 25% O_2 partial pressure were recorded as 3.1×10^{-4} Ω cm and 6.0×10^{-4} Ω cm. The resistivity values of SnO_2 films that were plasma oxidized at 50% O_2 partial pressure are 7.2×10^{-4} Ω cm, 4.8×10^{-4} Ω cm and 1.08×10^{-5} Ω cm for substrate temperatures of 100 °C, 150 °C, and 200 °C, respectively. Increasing the substrate temperature could lead to increased grain sizes and improved crystallinity of the SnO_2 films.

Consequently, a higher substrate temperature could lead to the formation of lower resistance or higher conductivity films because of the increase in mobility and/or carrier density at higher substrate temperatures [12].

4. Conclusions

Nanocrystalline tin films with a grain size of 34 nm were deposited onto stainless steel substrates in a 1.0 Pa

argon atmosphere from a metallic pure tin target using the thermal evaporation technique. Different tin oxide structures and morphologies were produced by changing the partial pressure of O_2 and the substrate temperature during plasma oxidation. Increasing the substrate temperature resulted in more crystalline structures for both the SnO and SnO_2 films. Plasma oxidized pure Sn coatings at 12.5% O_2 partial pressure exhibited a tetragonal SnO structure. Plasma oxidized pure Sn coatings for 12.5% O_2 exhibited equiaxed nanograins (43.06 nm) at 100 °C, but the morphology changed to a flower-like geometry when the substrate temperature increased to 150 °C (36.01 nm) and 200 °C (29.0 nm). Increasing the O_2 partial pressure to 25% and 50% resulted in a conversion to the cassiterite SnO_2 phase with grain sizes between 13.0 and 17.37 nm and without the SnO structure. Increasing substrate temperature resulted in increasing grain size. The electrical resistivity of the SnO_2 films is in the range of $7.2\times10^{-4}-1.08\times10^{-5}$ Ω cm. The resistivity values decreased with increasing substrate temperature.

Acknowledgments

The authors would like to acknowledge the financial support of Scientific and Technical Research council of Turkey (TUBITAK) under the contract no. 109M464.

References

[1] Q. Liu, Z. Liu, L. Feng, *Comput. Mater. Sci.* **47**, 1016 (2010).

[2] J.H. Shin, J.Y. Song, Y.H. Kim, H.M. Park, *Mater. Lett.* **64**, 1120 (2010).

[3] R.Y. Korotkov, P. Ricou, A.J.E. Farran, *Thin Solid Films* **502**, 79 (2006).

[4] M. Alaf, M.O. Guler, D. Gultekin, M. Uysal, A. Alp, H. Akbulut, *Vacuum* **83**, 292 (2009).

[5] H. Uchiyama, H. Imai, *Cryst. Growth Des.* **7**, 841 (2007).

[6] S. Wang, S. Xie, H. Li, S. Yan, K. Fan, M. Qiao, *Chem. Commun.*, 507 (2005).

[7] Y. Pei, S. Wang, Q. Zhou, S.-H. Xie, M.-H. Qiao, Z.-Y. Jiang, K.-N. Fan, *Chin. J. Chem.* **25**, 1385 (2007).

[8] H. Uchiyama, H. Imai, *Langmuir* **24**, 9038 (2008).

[9] Z. Jia, L. Zhu, G. Liao, Y. Yu, Y. Tang, *Solid State Commun.* **132**, 79 (2004).

[10] A. Yadav, E.U. Masumdar, A.V. Moholkar, M. Neumann-Spallart, K.Y. Rajpure, C.H. Bhosale, *J. Alloys Comp.* **488**, 350 (2009).

[11] S.J. Ikhmayies, R.N.A. Bitar, *Mater. Sci. Semicond. Proc.* **12**, 122 (2009).

[12] V. Senthilkumar, P. Vickraman, *Curr. Appl. Phys.* **10**, 880 (2010).